

Structure and Function of the $\beta 2$ Subunit of Brain Sodium Channels, a Transmembrane Glycoprotein with a CAM Motif

L. L. Isom,* D. S. Ragsdale, K. S. De Jongh,†
R. E. Westenbroek, B. F. X. Reber,‡ T. Scheuer,
and W. A. Catterall

Department of Pharmacology
University of Washington
Seattle, Washington 98195-7280

Summary

Voltage-gated sodium channels in brain neurons are complexes of a pore-forming α subunit with smaller $\beta 1$ and $\beta 2$ subunits. cDNA cloning and sequencing showed that the $\beta 2$ subunit is a 186 residue glycoprotein with an extracellular NH_2 -terminal domain containing an immunoglobulin-like fold with similarity to the neural cell adhesion molecule (CAM) contactin, a single transmembrane segment, and a small intracellular domain. Coexpression of $\beta 2$ with α subunits in *Xenopus* oocytes increases functional expression, modulates gating, and causes up to a 4-fold increase in the capacitance of the oocyte, which results from an increase in the surface area of the plasma membrane microvilli. $\beta 2$ subunits are unique among the auxiliary subunits of ion channels in combining channel modulation with a CAM motif and the ability to expand the cell membrane surface area. They may be important regulators of sodium channel expression and localization in neurons.

Introduction

Voltage-gated sodium channels are the membrane proteins responsible for the rising phase of the action potential in most excitable cells, including nerve, skeletal muscle, heart, and neuroendocrine tissues (Hille, 1992). Sodium channels isolated from rat brain are a heterotrimeric complex composed of a 260 kDa pore-forming α subunit and two smaller auxiliary β subunits, $\beta 1$ (36 kDa) and $\beta 2$ (33 kDa) (reviewed by Catterall, 1992; Isom et al., 1994). $\beta 1$ has been shown to be noncovalently associated with α , while $\beta 2$ is covalently linked by disulfide bonds. The $\beta 1$ subunit is a glycoprotein with a single membrane-spanning segment (Isom et al., 1992). Coexpression of sodium channel α and $\beta 1$ subunits results in increases in the rates of activation and inactivation, a shift from slow to fast gating mode, hyperpolarizing shifts in the voltage dependence of activation and inactivation, and an increase in sodium channel expression (Isom et al., 1992, 1995; Bennett et al., 1993; Patton et al., 1994; Makita

et al., 1994). Moreover, adult rat brain $\beta 1$ subunits can modulate multiple α subunit isoforms from brain, skeletal muscle, and heart (Patton et al., 1994; Isom et al., 1995; Makita et al., 1994; Cannon et al., 1993; Tong et al., 1993; Qu et al., 1995).

In contrast with $\beta 1$ subunits, $\beta 2$ subunits are only observed in neuronal sodium channels (Wollner et al., 1987). Formation of the disulfide-linked complex of α and $\beta 2$ subunits occurs late in the assembly process and is correlated with insertion of the mature sodium channel into the cell surface (Schmidt and Catterall, 1986, 1987). Disulfide linkage to $\beta 2$ subunits accompanies large increases in sodium channel density in developing brain and retina (Scheinman et al., 1989; Wollner et al., 1988). Thus, $\beta 2$ subunits may function as important regulators of sodium channel expression in neurons, but their structure and the molecular basis for their interactions with α subunits have been unknown.

Results

Cloning of a $\beta 2$ cDNA

To define the structure of the $\beta 2$ subunits, rat brain sodium channels were purified (Hartshorne and Catterall, 1984), $\beta 2$ subunits were isolated and separated by SDS-polyacrylamide gel electrophoresis (SDS-PAGE) (Messner and Catterall, 1986; Reber and Catterall, 1987), and the NH_2 -terminal sequence was determined to be MEVTVPT-TLSVL?GSDTR as described in the Experimental Procedures. Peptide fragments of the $\beta 2$ subunit were prepared by digestion with trypsin or V8 protease, and amino acid sequences of seven peptides were determined (see underlined sequences in Figure 2B). To verify that the NH_2 -terminal sequence was indeed that of the $\beta 2$ subunit, a peptide was synthesized corresponding to amino acids 2–14 with W at position 13 and KY at the NH_2 -terminal end, coupled to bovine serum albumin, and used for production of a polyclonal antiserum as previously described (Gordon et al., 1988). Antibodies from this serum recognized a single protein band in purified sodium channel preparations in the position of the $\beta 2$ subunit (Figure 1A). This protein band comigrated with the α subunit and the saxitoxin-binding activity of the sodium channel complex in sucrose gradient sedimentation, confirming its identification as the $\beta 2$ subunit (Figures 1B and 1C).

To isolate cDNA clones encoding the rat brain sodium channel $\beta 2$ subunit, we initially amplified a 90 bp cDNA encoding 30 amino acids of a $\beta 2$ peptide by polymerase chain reaction (PCR) using $\beta 2$ -specific degenerate oligonucleotides. Two cDNA clones of 300 bp and 303 bp were then isolated by PCR with overlapping oligonucleotide primers as described in the Experimental Procedures. These two clones were used to screen 500,000 recombinants from a rat brain cDNA library. A single clone of approximately 3000 bp, p $\beta 2.8a-1$ (Figure 2A), was isolated and analyzed to determine the nucleotide sequence encoding the $\beta 2$ protein.

*Present address: Department of Pharmacology, University of Michigan School of Medicine, Ann Arbor, Michigan 48109-0632.

†Present address: Cell Therapeutics, 201 Elliott Avenue, Suite 400, Seattle, Washington 98119

‡Present address: Institute of Pharmacology, University of Bern, 3010 Bern, Switzerland.

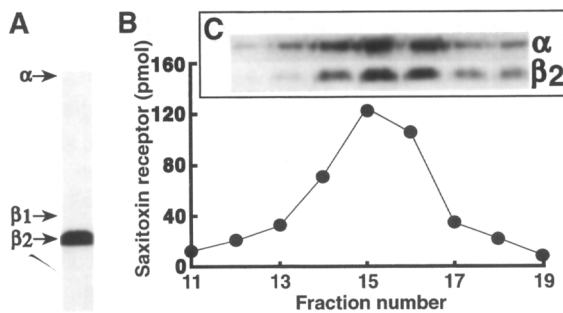


Figure 1. Immunospecific Identification of $\beta 2$ Subunits

(A) Purified sodium channels were analyzed by immunoblotting with the antibody to the NH_2 -terminal sequence of purified $\beta 2$ subunits, anti- $\beta 2$ -1. For detection of the α and $\beta 2$ subunits by immunoblotting, SDS-PAGE was carried out under reducing conditions in 10% polyacrylamide gels. Electrophoresis to nitrocellulose and immunostaining with ^{125}I -labeled protein A were carried out as described previously (De Jongh et al., 1989). The migration positions of the α , $\beta 1$, and $\beta 2$ subunits on silver-stained gels are shown by arrows.

(B) Rat brain sodium channels purified by ion exchange, hydroxylapatite, and wheat germ agglutinin affinity chromatography were fractionated by sucrose gradient sedimentation, and aliquots from each fraction were analyzed for [^3H]saxitoxin binding by rapid gel filtration (Hartshorne and Catterall, 1984).

(C) Fractions from the same sucrose gradient sedimentation were analyzed by immunoblotting with antibodies directed against the α and $\beta 2$ subunits.

The sequence of the coding region of the $\beta 2$ genomic DNA was determined by amplification using oligonucleotides encoding the 5' and 3' ends of the $\beta 2$ coding region as templates for PCR and cDNA sequencing. This procedure resulted in the isolation of a genomic fragment of 1349 bp (Figure 2A) that contained the $\beta 2$ coding region interrupted by two introns. No evidence was found for alternate coding sequences within these two introns. A single allelic difference (T to G) within the coding sequence of the genomic fragment was observed that changes Phe-51 encoded in the cDNA clone to a valine in the genomic DNA.

Primary Structure of $\beta 2$

The deduced amino acid sequence of $\beta 2$ revealed two potential translation start sites (positions -29 and 1), as illustrated in Figure 2B. The methionine shown at position 1 was the residue observed in the first cycle of NH_2 -terminal amino acid sequencing and, therefore, is the first residue of the mature $\beta 2$ subunit isolated from adult rat brain. Its codon is surrounded by a satisfactory Kozak sequence (Kozak, 1986). An upstream alternative translation start site (methionine at position -29) also has a satisfactory Kozak sequence and predicts a precursor protein that contains a 29 residue cleaved NH_2 -terminal signal peptide. As shown below (see Figure 4), only the protein with the signal peptide was functionally expressed in *Xenopus* oocytes, indicating that the methionine at position -29 is the correct translation start site. The $\beta 2$ cDNA clones thus contain a 645 bp open reading frame coding for 215 amino acids. This sequence includes the NH_2 -terminal sequence of the mature $\beta 2$ protein as well as six additional peptide sequences determined by amino acid sequencing (underlined in Figure 2B).

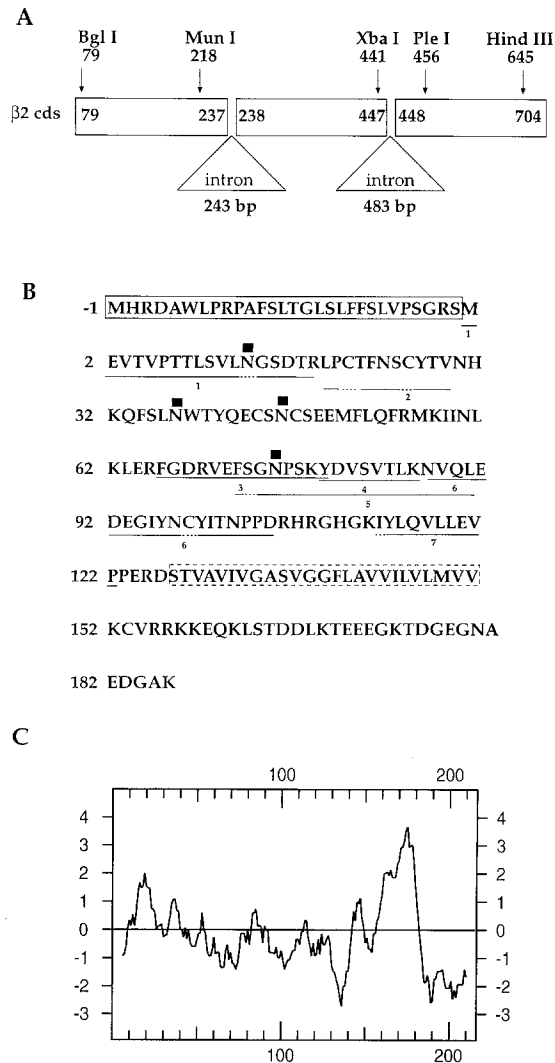


Figure 2. Molecular Cloning and Sequencing of $\beta 2$ Subunit cDNA

(A) cDNAs complementary to $\beta 2$ mRNA and to the $\beta 2$ genomic DNA were cloned and sequenced as described in the Experimental Procedures. The structure of the $\beta 2$ cDNA and the positions of introns and representative restriction sites in the coding sequence are illustrated. (B) Deduced amino acid sequence of the $\beta 2$ subunit. Predicted amino acid sequence corresponding to the experimentally determined NH_2 -terminal amino acid sequence (peptide 1) and peptides generated by trypsin (peptides 2, 3, 4, 6, and 7) and V8 protease (peptide 5) are indicated by solid underlines. Dotted underlines indicate residues that were ambiguous by amino acid sequencing. The putative cleaved signal sequence is indicated by the solid box. The predicted transmembrane segment is indicated by the dotted box. Predicted N-linked glycosylation sites are marked by closed squares.

(C) Hydrophobicity analysis of deduced amino acid sequence of $\beta 2$ computed according to Kyte and Doolittle (1982). The window size is six residues plotted at one residue intervals.

The molecular mass calculated from the deduced amino acid sequence excluding the cleaved signal peptide is 20,902 daltons, which is in close agreement with the observed molecular mass of 21 kDa for the deglycosylated $\beta 2$ subunit as determined by SDS-PAGE (Messner and Catterall, 1985). Hydrophobicity analysis (Kyte and Doolittle, 1982) of the $\beta 2$ precursor predicted a NH_2 -terminal

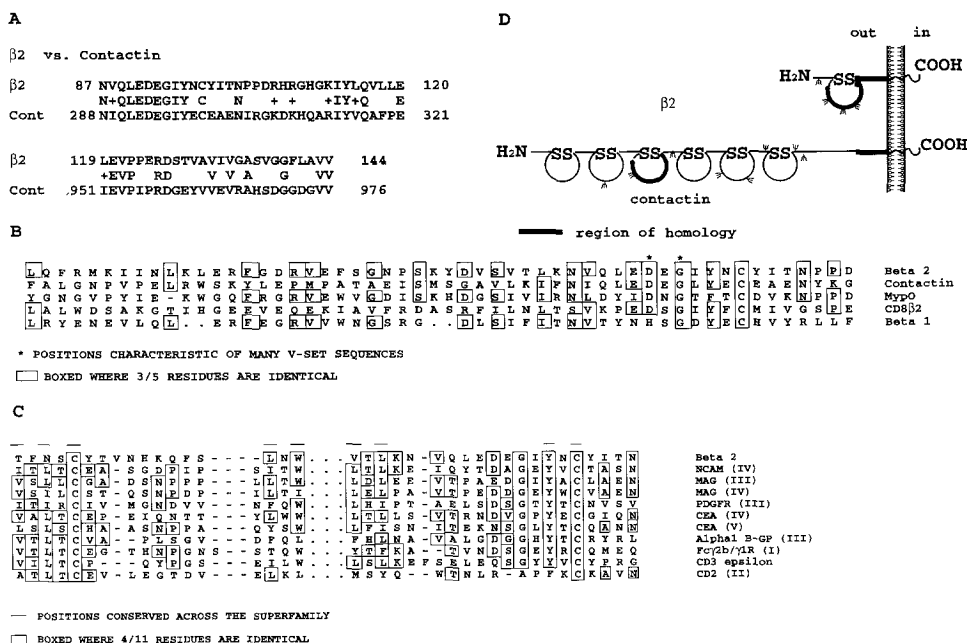


Figure 3. Amino Acid Sequence Similarity of $\beta 2$ Subunit with Contactin and Other Immunoglobulin Superfamily Members

(A) Amino acid sequences of mouse F3/contactin (Gennarini et al., 1989) are compared with $\beta 2$ in the region of high sequence similarity; identical residues are indicated on the central line, and positions of homologous substitutions are indicated by a plus. The sequence numbers reflect the mature form of $\beta 2$ and the precursor form of F3/contactin.

(B) Comparison of the amino acid sequences of the $\beta 2$ subunit ($\beta 2$), contactin, and proteins with V-type immunoglobulin folds (V-SET). The accession numbers and residue numbers for the amino acid sequences are as follows: sodium channel $\beta 2$ subunit, residues 52–105; contactin, P14781 and P10450, residues 255–308; myelin p0 protein (Myp0), P02938, residues 80–132; $\beta 2$ chain of CD8 (CD8 $\beta 2$), Q00954, residues 69–122; sodium channel $\beta 1$ subunit ($\beta 1$), P14860, residues 52–109. Positions that are predictive for V-SET sequences are noted by an asterisk (Williams and Barclay, 1988).

(C) Comparison of the amino acid sequences of the $\beta 2$ subunit and representative C2-SET proteins taken from Williams and Barclay (1988). Positions that are conserved across the superfamily of immunoglobulin domains are indicated by a line above the sequence position. The amino acid residues illustrated are as follows: $\beta 2$, residues 22–102; NCAM, residues 306–370; myelin-associated glycoprotein (MAG), residues 257–309 and 343–396; platelet-derived growth factor receptor (PDGFR), residues 199–263; carcinoembryonic antigen (CEA), residues 307–363 and 360–447; $\alpha 1$ β -glycoprotein (alpha1 B-GP), residues 206–261; Fc γ 2b/y1 receptor (Fc γ 2b/y1R), residues 24–104; lymphocyte antigen CD3 ϵ (CD3 epsilon), residues 17–74; lymphocyte antigen CD2, residues 113–161. Original references to articles describing these proteins are given by Williams and Barclay (1988).

(D) The predicted structures of the $\beta 2$ subunit and contactin illustrating the predicted disulfide bond between Cys-26 and Cys-98 of $\beta 2$, the immunoglobulin folds and consensus sequences for glycosylation (Y) of both molecules, and the sequences with homology between the two molecules.

signal peptide and a single transmembrane segment spanning residues 128–151 (Figure 2C). Thus, the predicted membrane topology of $\beta 2$ is type I, with a large extracellular NH₂-terminal domain, a single transmembrane segment, and a short intracellular COOH-terminal domain (Wickner and Lodish, 1985). The predicted extracellular domain of $\beta 2$ contains four consensus sequences for N-linked glycosylation, in agreement with biochemical results (Messner and Catterall, 1985). The predicted membrane topology and glycosylation pattern of the $\beta 2$ subunit closely resemble the $\beta 1$ subunit of sodium channels (Isom et al., 1992). Comparison of the amino acid sequences of these two auxiliary subunits does not reveal any contiguous sequence similarities, but both are predicted to form extracellular immunoglobulin-like folds (see below).

Similarity to Contactin and the Immunoglobulin Superfamily

A comparison of the deduced amino acid sequence of the $\beta 2$ subunit with sequences in the GenPept and SwissProt

databases revealed an interesting sequence similarity with two separate segments of the neural cell adhesion molecule (CAM) contactin (also called neural cell surface protein F3 in mouse), a membrane glycoprotein of the immunoglobulin superfamily (Ranscht, 1988; Gennarini et al., 1989; Figure 3A). One sequence of 34 residues in the extracellular domain of $\beta 2$ (residues 87–120 of the mature $\beta 2$ protein) is 45% identical to a segment in the NH₂-terminal one third of contactin/F3 (residues 288–321 of the contactin precursor) with no inserted gaps. This sequence begins on the COOH-terminal side of the four consensus sites for N-linked glycosylation of $\beta 2$. The following sequence of 25 residues of $\beta 2$ (residues 120–144) is 42% identical to a sequence near the COOH-terminal of contactin (residues 951–976) (Figure 3A). These striking similarities in amino acid sequence suggest a structural and functional relationship between the $\beta 2$ subunit and contactin/F3.

Because the first segment of amino acid sequence similarity is located within the third of six C2-type immunoglob-

ulin repeats in the extracellular domain of contactin, we examined whether the extracellular domain of $\beta 2$ also is predicted to form an immunoglobulin repeat using the ALIGN algorithm (Dayhoff et al., 1983) and the criteria defined by Williams and Barclay (1988). This analysis predicts that the extracellular domain of the $\beta 2$ subunit forms a single immunoglobulin repeat with a disulfide bond between Cys-26 (or possibly Cys-21) and Cys-98. The conserved segments of the immunoglobulin repeat surrounding Cys-98 in $\beta 2$ are compared with the corresponding regions of contactin and a few V-type immunoglobulin repeats in Figure 3B. The predicted structure of the $\beta 2$ immunoglobulin fold is most closely related to that of myelin protein p0, the principal protein of myelin (Z score = 8.7 SD). p0 is thought to be involved in homophilic interactions between layers of wrapped myelin sheaths in peripheral nerves. The immunoglobulin fold of $\beta 2$ is also significantly related in predicted structure to immunoglobulin G (IgG) heavy chain (Z score = 6.8 SD), the lymphocyte CAM CD8 (Z score = 4.8 SD), and contactin/F3 (Z score = 3.6 SD). The $\beta 2$ sequence with similarity to contactin (residues 87–120) is located at the COOH-terminal end of the predicted immunoglobulin fold of $\beta 2$, similar to the position of the corresponding sequence in the third immunoglobulin repeat of contactin (Gennarini et al., 1989). This comparison suggests the possibility that this segment of $\beta 2$ may have a similar structure to the third immunoglobulin repeat of contactin.

The $\beta 1$ subunit of sodium channels has a similar transmembrane topology to $\beta 2$ (Isom et al., 1992). Analysis of the $\beta 1$ sequence with the ALIGN algorithm also reveals an immunoglobulin fold in its extracellular domain. Its predicted structure is significantly related to that of $\beta 2$ (Z score = 4.2 SD), although not as closely related as myelin p0, IgG heavy chain, CD8 (Figure 3B), and many other proteins not listed here (unpublished data). As for $\beta 2$, several conserved residues among proteins with V-type immunoglobulin folds are present in $\beta 1$ in positions appropriate for formation of a V-type immunoglobulin fold (Figure 3B).

Many other CAMs have immunoglobulin folds of the C2 type in their extracellular domains including neural CAM (NCAM) and myelin-associated glycoprotein (MAG) (Williams and Barclay, 1988). Although the predicted structures of these proteins are not as closely related to $\beta 2$ as those with V-type immunoglobulin folds described above, many of the amino acid residues that are conserved among these CAMs with C2-type immunoglobulin repeats are also conserved in $\beta 2$ (Figure 3C), consistent with the conclusion that the $\beta 2$ subunit contains a CAM motif in its extracellular domain.

In contactin/F3, the second segment of sequence similarity with $\beta 2$ is separated from the first by 630 amino acid residues (Figure 3D). It is located in the membrane-proximal domain of the contactin/F3 molecule, immediately on the NH₂-terminal side of the glycoposphatidylinositol anchor of mouse contactin/F3. The corresponding segment of $\beta 2$ is also proximal to the membrane and extends from the predicted immunoglobulin fold into the pre-

dicted transmembrane segment. Thus, in the structure of $\beta 2$ (Figure 3D), a short NH₂-terminal glycosylated segment with no sequence similarity to known proteins is followed by an immunoglobulin fold containing a segment with sequence similarity to the extracellular matrix-binding domain of contactin/F3. This immunoglobulin fold is connected directly to a segment with sequence similarity to the membrane-proximal domain of contactin/F3 that extends into the predicted transmembrane segment of $\beta 2$. The striking similarity to the amino acid sequence of contactin/F3 suggests that the extracellular domain of the $\beta 2$ subunit may serve a function in cell–cell interaction during development in addition to the role of $\beta 2$ in modulation of sodium channel function.

Functional Expression of $\beta 2$ in *Xenopus* Oocytes

To investigate the effects of the $\beta 2$ subunit on sodium channel expression and function, we injected *Xenopus* oocytes with in vitro transcribed RNA encoding either the putative precursor form or the mature form of $\beta 2$ together with RNA encoding the type IIA sodium channel α subunit and the $\beta 1$ subunit in various combinations and examined the properties of the expressed sodium channels with two-microelectrode voltage clamp recording. The RNA encoding the mature form of $\beta 2$ had no detectable effect on the expression levels or functional properties of sodium channels in oocytes. In contrast, coexpression of the precursor form of $\beta 2$ along with α alone or with α plus $\beta 1$ resulted in an increase in the amplitude of whole-cell sodium currents across a wide range of test pulse potentials (Figure 4A). These results support the conclusion that the methionine residue at position –29 is the correct translation start site. $\beta 2$ did not shift the current–voltage relationship (Figure 4A), indicating that the larger currents in the presence of $\beta 2$ were caused by an increase in channel expression rather than a change in the voltage dependence of channel activation. In contrast, $\beta 2$ did cause a small, but significant negative shift in the voltage dependence of steady-state inactivation (Figure 4B).

The effect of $\beta 2$ subunits on sodium channel expression was concentration dependent. Sodium currents recorded from oocytes injected with equal amounts of α and $\beta 2$ RNA were 1.8 times larger than currents in oocytes expressing α alone, whereas the currents were 2.9-fold larger in oocytes injected with a 5-fold weight ratio of $\beta 2$: α RNA (Figure 4C). Injection of $\beta 2$ alone did not result in detectable sodium currents, indicating that $\beta 2$ did not up-regulate endogenous sodium channels in oocytes. $\beta 1$ subunits increased sodium channel expression about 2.3-fold (Figure 4C), as previously reported (Isom et al., 1992). Coexpression of α , $\beta 1$, and $\beta 2$ resulted in a 3.7-fold increase in current, a larger effect than seen when α was expressed with either $\beta 1$ or $\beta 2$ alone. Thus, the most efficient expression of sodium channels was obtained when RNA encoding the full complement of subunits was injected into oocytes.

To examine the effects of $\beta 2$ on the kinetics of sodium channel activation and inactivation, we recorded macroscopic sodium currents in cell-attached macropatches to

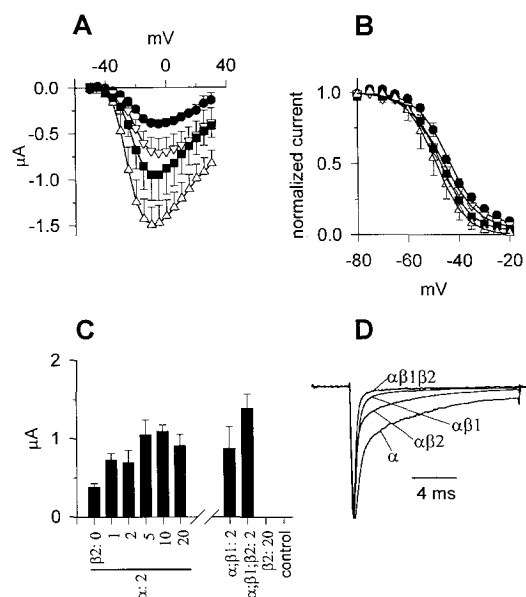


Figure 4. Effects of β2 Subunits on Sodium Channel Expression and Function

The data shown in (A)–(C) were obtained from two-electrode voltage-clamp recordings.

(A) Current–voltage relationships. Sodium currents were evoked by 30 ms long depolarizations to varying test potentials, from a holding potential of -90 mV. The graph shows the mean \pm SEM amplitudes of peak sodium currents, plotted as a function of test potential for oocytes expressing α (closed circles; $n = 7$), $\alpha\beta 2$ (inverted triangles; $n = 5$), $\alpha\beta 1$ (closed squares; $n = 5$), and $\alpha\beta 1\beta 2$ (triangles; $n = 5$). RNAs encoding all subunits were injected at 2 ng/ml.

(B) Steady-state inactivation curves. Currents were elicited by a test pulse to 0 mV after a 100 ms long prepulse to varying potentials. The graph shows the mean amplitudes \pm SEM of the currents evoked by the test pulse as a function of the prepulse potential, normalized with respect to the currents elicited after a prepulse to -80 mV. The data were obtained from the same oocytes as in (A), and the symbols have the same meaning. The smooth lines through the data points are according to $1/(1 + \exp[(V_m - V_{1/2})/s])$, where V_m is the prepulse potential and $V_{1/2}$ and s have the following values: circles, -44.2 mV and 6.2 mV; inverted triangles, -46.2 mV and 7.0 mV; squares, -47.3 mV and 5.9 mV; triangles, -48.8 mV and 5.8 mV.

(C) Dependence of current amplitude on $\beta 2$ concentration. The graph shows the mean amplitude \pm SEM of currents elicited by depolarization to 0 mV from a holding potential of -90 mV in oocytes injected with 50 nl of the indicated concentrations (in nanograms per microliter) of α , $\beta 1$, and $\beta 2$ RNA. The means shown by each bar were obtained from (left to right) 7 , 6 , 5 , 6 , 7 , 7 , 6 , 5 , 3 , and 2 oocytes respectively.

(D) Effects of $\beta 2$ subunits on current time course in cell-attached macropatches. Each trace shows the mean currents elicited by depolarization to 0 mV from a holding potential of -140 mV for patches obtained from oocytes expressing α ($n = 7$ patches), $\alpha\beta 2$ ($n = 6$), $\alpha\beta 1$ ($n = 5$), and $\alpha\beta 1\beta 2$ ($n = 3$). The mean currents were determined in each condition and then the records were normalized so that the peak currents were the same amplitude.

achieve better time resolution. With strong depolarizations, sodium currents in macropatches from oocytes expressing either α , $\alpha\beta 1$, $\alpha\beta 2$, or $\alpha\beta 1\beta 2$ activated rapidly, but they exhibited very different time courses of inactivation (Figure 4D). In patches expressing α alone, the inactivation time course had two distinct components, a fast phase and a prominent slow phase that accounted for more than 50% of the current. These different components of inactivation

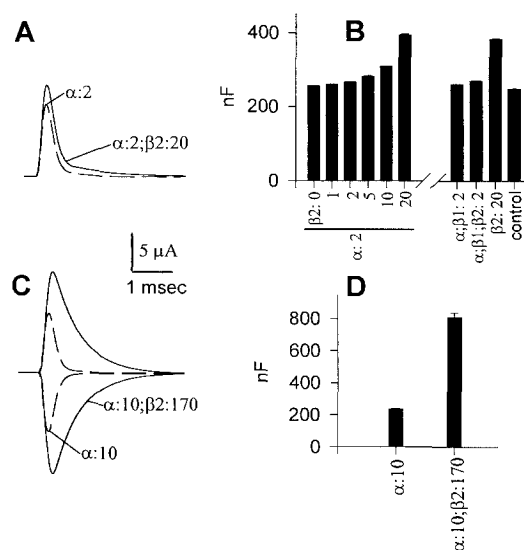


Figure 5. β2 Expression Increases Cell Capacitance in Xenopus Oocytes

(A) Typical capacity transients in oocytes injected with 2 ng/ μ l α RNA, either alone (dotted trace) or with 20 ng/ μ l $\beta 2$ RNA (solid trace). Transients were obtained using two-electrode voltage-clamp recording, by stepping the membrane potential to -60 mV from a holding potential of -90 mV.

(B) Mean \pm SEM capacitances of oocytes injected with varying concentrations of α , $\beta 1$, and $\beta 2$. Capacitance values were determined by integrating transients like the ones shown in (A). The concentrations of the RNAs encoding the subunits in nanograms per microliter are listed below the graph. Means were obtained from 7 , 7 , 5 , 6 , 7 , 7 , 6 , 6 , 4 , and 2 experiments, respectively.

(C) Typical capacity traces in oocytes from a different frog, injected with 10 ng/ μ l α subunit RNA, either alone (dashed trace) or with 170 ng/ μ l $\beta 2$ RNA (solid trace). Capacitive transients were obtained using two-electrode voltage-clamp recording, by stepping the membrane potential to -60 mV or -120 mV from a holding potential of -90 mV.

(D) Mean \pm SEM capacitances of oocytes injected with 10 ng/ μ l α subunit RNA, either alone ($n = 2$) or with 170 ng/ μ l $\beta 2$ RNA ($n = 2$).

reflect subpopulations of sodium channels in fast and slow gating modes (Krafte et al., 1990; Moorman et al., 1990; Zhou et al., 1991). As has been previously shown (Isom et al., 1992; Patton et al., 1994; Makita et al., 1994), coexpression of $\beta 1$ with α accelerated the inactivation time course by shifting most channels to a fast gating mode. Coexpression of $\beta 2$ also increased the proportion of fast gating channels, although to a lesser extent than $\beta 1$. The fastest currents were seen when α , $\beta 1$, and $\beta 2$ were expressed together. In this case, there was virtually no slow component in the time course of inactivation. These results show that $\beta 2$ promotes fast gating of sodium channels expressed in oocytes as well as increases the level of functional expression.

Increased Cell Membrane Surface Area Caused by Expression of β2 Subunits

A surprising, but highly reproducible effect of $\beta 2$ was a concentration-dependent increase in the whole-cell capacitance (Figures 5A and 5B). The cell capacitance is proportional to the integral of the capacitance current transient recorded following a change in voltage in the voltage

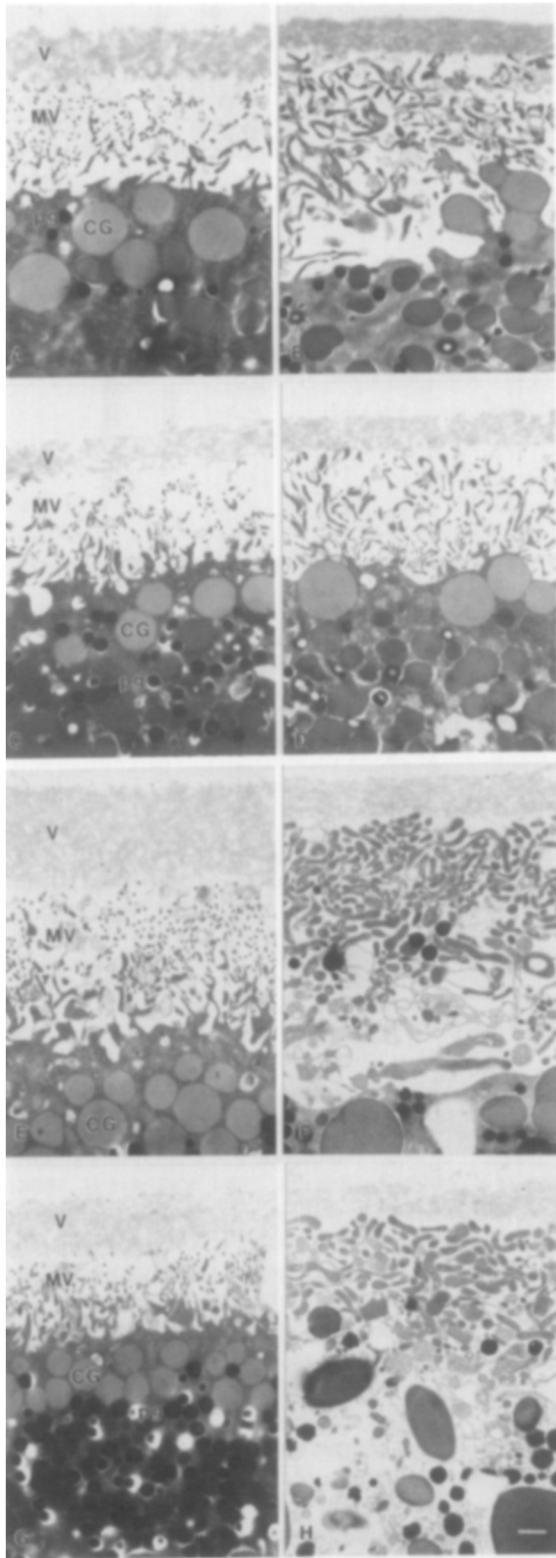


Figure 6. $\beta 2$ Expression Increases Cell Surface Area
Electron micrographs of un.injected oocytes and $\beta 2$ -injected oocytes were taken as described in the Experimental Procedures. (A, C, E, and G) Sections from control oocytes, demonstrating the normal ultrastructure of the oocyte. V, vitelline membrane; MV, microvilli; CG, cortical granules; pg, pigment granules. (B) A section from an oocyte comparable to (A) fixed 2 days following

clamp. This integral is clearly increased when $\beta 2$ subunits are expressed (Figure 5A). An increase in capacitance was first observed with injection of 5 ng/ μ l $\beta 2$ RNA, and progressively larger increases were observed with higher concentrations of $\beta 2$ RNA (Figure 5B). Since cell capacitance is directly proportional to cell surface area (approximately 1 cm² per μ F), these results indicate that $\beta 2$ causes an increase in the surface area of the external plasma membrane of the oocyte. This increase in capacitance was not observed in oocytes injected with α or $\alpha\beta 1$ RNA, but was consistently seen in oocytes injected with $\alpha\beta 2$, $\alpha\beta 1\beta 2$, or $\beta 2$ RNA alone (Figure 5B). The maximum increase in sodium channel expression was observed with 5 ng/ μ l $\beta 2$ RNA (see Figure 4C). This concentration of $\beta 2$ RNA caused only a 10% increase in membrane capacitance (Figure 5B). Therefore, the increase in functional expression of sodium channels by $\beta 2$ subunits is not caused by a general increase in the area of the cell surface membrane.

Injection of higher concentrations of $\beta 2$ mRNA caused dramatic increases in the capacitance of the oocyte, indicating a substantial expansion of membrane surface area (Figure 5C). Up to a 4-fold increase in cell surface capacitance was observed with injection of 170 ng/ μ l $\beta 2$ RNA (Figure 5D). The increase in capacitance was similar when measured with either depolarizing or hyperpolarizing test pulses (Figure 5C) and when studied in oocytes expressing $\beta 2$ subunits only or functional sodium channels containing α , $\beta 1$, and $\beta 2$ subunits (Figure 5B). These results indicate that neither voltage-gated ion channels endogenous to the oocyte nor exogenously expressed sodium channels affect the capacitance measurement. In contrast with the large increase in capacitance, no significant change in the size or shape of these oocytes was observed in the light microscope. Thus, the increased membrane surface area must be accommodated by increased folding of the plasma membrane rather than by increased volume of the cell.

To examine directly whether the cell surface membrane of oocytes expressing $\beta 2$ subunits was more highly folded, we examined control, $\beta 1$ -injected, and $\beta 2$ -injected oocytes by electron microscopy after 2 and 4 days in vitro (Figure 6). Control oocytes have a layered surface structure consisting of the external, proteoglycan vitelline membrane (V), the highly folded plasma membrane containing numer-

injection of 300 ng/ μ l $\beta 2$ RNA, illustrating an apparent increase in the relative density and size of microvilli and the protrusion of cortical granules into the microvillus layer.

(D) A section from an oocyte comparable to (C) injected with 300 ng/ μ l $\beta 2$ RNA 2 days prior to fixation, demonstrating an overall increase in the relative size and density of microvilli and the presence of cortical granules just beneath the surface membrane.

(F) A section from a $\beta 2$ -injected oocyte comparable to (E), fixed 4 days after injection, demonstrating the density and thickness of the microvillus layer, the thinning of the vitelline envelope, and the absence of cortical granules.

(H) A section from a $\beta 2$ -injected oocyte comparable to (G), illustrating that $\beta 2$ expression results in an overall increase in relative density and size of microvilli associated with the surface membrane. Scale bar, 10 μ m.

ous microvilli (MV), the submembrane cortical granules (CG), and the dark pigment granules (pg) (Figures 6A, 6C, 6E, and 6G). The thickness of the microvillus layer increases with distance from the equator of the oocyte (compare Figures 6A and 6C), so we have compared sections of control and injected oocytes from comparable locations close to and distant from the equator in each pair of photos in Figure 6. Oocytes injected with $\beta 1$ RNA (300 ng/ μ l) are unchanged from controls (data not shown). In contrast, 2 days after injection of $\beta 2$ RNA, there is a striking increase in the number and size of microvilli in the plasma membrane and a noticeable reduction in the number of cortical granules lying under the plasma membrane (Figures 6B and 6D). In some sections, cortical granules are observed fusing with protrusions of the cell surface membrane (Figure 6B). By 4 days after injection, the increase in the number and surface area of the microvilli is even more apparent, the microvillus layer is considerably thicker than in controls, few cortical granules are observed in the submembrane region, and the number of pigment granules also appears to be reduced (Figures 6F and 6H). Often the vitelline membrane appears thinner in $\beta 2$ -injected oocytes, suggesting that it is stretched to accommodate the increased size of the microvillus layer (Figures 6F and 6H). These results confirm the conclusion from the capacitance studies that $\beta 2$ subunits cause an increase in the plasma membrane surface area and in its folding into microvilli. They also suggest that $\beta 2$ exerts these effects by increasing the fusion of intracellular membrane vesicles with the plasma membrane. These may include vesicles containing newly synthesized sodium channels at low levels of $\beta 2$ expression and the endogenous cortical granules and pigment granules of the oocyte at higher levels of $\beta 2$ expression.

Expression of $\beta 2$ During Neural Development

To examine the tissue-specific expression of mRNAs encoding the sodium channel $\beta 2$ subunit, we isolated total RNA from various rat tissues and subjected it to Northern blot analysis. A strongly hybridizing band of approximately 4.3 kb was detected in rat brain and rat spinal cord but not in rat liver, heart, or skeletal muscle (Figure 7A). Overexposure of the Northern blots did not reveal any further hybridization signal, suggesting that $\beta 2$ is expressed primarily or exclusively in the nervous system, in agreement with previous biochemical data (Wollner et al., 1987).

RNA samples from electric eel brain and electroplax were also examined as representative tissues from a non-mammalian vertebrate species whose sodium channels are biochemically well characterized (Levinson et al., 1986). Sodium channels in eel electroplax have only α subunits (Levinson et al., 1986); $\beta 2$ subunits are not detected in either eel electroplax or brain with antibodies against purified rat brain $\beta 2$ (Wollner et al., 1987). Consistent with the results of the previous biochemical experiments, $\beta 2$ mRNA was not detected in either eel electroplax or brain. Either $\beta 2$ is not present in eel or its sequence is highly divergent from rat.

$\beta 2$ is not expressed uniformly in all areas of the brain (Figure 7B). A strong signal was observed in cerebral cor-

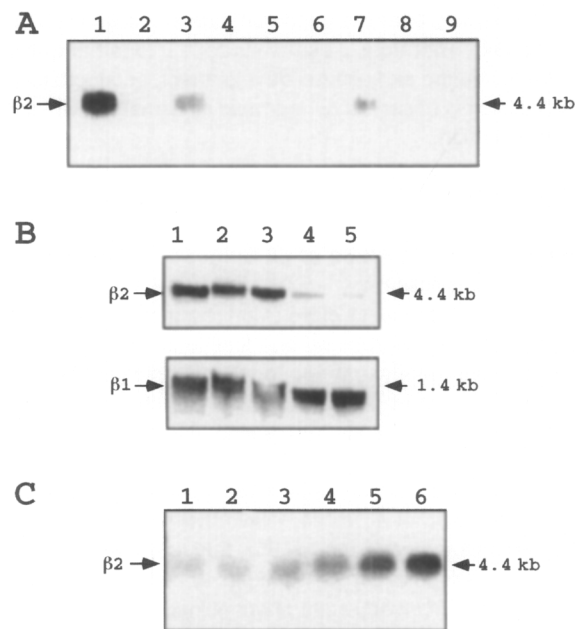


Figure 7. Tissue-Specific Expression of $\beta 2$ Subunit mRNA

(A) Northern blot analysis of total RNA from various tissues using a specific $\beta 2$ subunit probe. We separated 10 μ g of each sample on an agarose-formaldehyde gel, blotted to nylon, and hybridized with a $\beta 2$ subunit-specific cRNA antisense probe. Lane 1, rat brain; lane 2, rat liver; lane 3, rat spinal cord; lane 4, rat adrenal; lane 5, rat heart; lane 6, rat skeletal muscle; lane 7, rat brain; lane 8, eel brain; lane 9, eel electroplax.

(B) Differential expression of $\beta 1$ and $\beta 2$ subunit mRNA in different brain regions. Lane 1, total brain; lane 2, cerebral cortex; lane 3, cerebellum; lane 4, hippocampus; lane 5, brain stem.

(C) Developmental time course of $\beta 2$ mRNA expression in rat brain. Total cellular RNA was isolated from rat brain at embryonic days 9, 15, and 20 or postnatal days 2, 7, and 14 (lanes 1–6). Northern blot analysis was performed using a $\beta 2$ subunit-specific cRNA antisense probe as described in the Experimental Procedures.

tex and cerebellum, a band of moderate intensity was seen in hippocampus, and a very weak signal was detected in brain stem. In contrast, $\beta 1$ subunits are expressed comparatively uniformly in the brain regions tested (Figure 7B). Previous biochemical data have shown that greater than 89% of all purified rat brain sodium channels contain a disulfide-linked $\beta 2$ subunit (Wollner et al., 1987). Thus, since $\beta 2$ expression does not parallel α subunit expression, these data suggest that more than one $\beta 2$ subunit isoform may exist in different regions of the central nervous system.

Expression of $\beta 2$ subunit mRNA is detectable by embryonic day 9 in the brain (Figure 7C), in contrast with $\beta 1$ subunits that are first detected after birth using comparable Northern blotting procedures (Patton et al., 1994). The level of $\beta 2$ mRNA remains relatively constant until birth and then rapidly increases to adult levels by postnatal day 14. Sodium channel α subunit mRNA is present in the brain at embryonic day 10 and greatly increases in amount following birth due to increased transcription (Scheinman et al., 1989; Wollner et al., 1988; Beckh et al., 1989). Neurogenesis in the rat central nervous system begins at embryonic day 9–10; axonal growth and synaptogenesis in-

crease rapidly after birth and continue at a high level for 2–3 weeks. Therefore, $\beta 2$ subunits appear together with α subunits during early neural development, and increased expression is observed during rapid neuronal growth and differentiation.

Discussion

Structure and Function of $\beta 2$ Subunits in Sodium Channel Expression

$\beta 2$ subunits represent a class of ion channel auxiliary subunits with unique structural and functional properties. Although their transmembrane topology, extent of N-linked glycosylation, and predicted overall structure resemble the $\beta 1$ subunits of sodium channels (Isom et al., 1992), no contiguous sequence similarities are apparent in comparisons with $\beta 1$ or with the auxiliary subunits of other ion channels (Isom et al., 1994). Nevertheless, both $\beta 1$ and $\beta 2$ subunits increase the level of functional expression, shift channels to a fast gating mode, and shift the voltage dependence of steady-state channel inactivation to more negative membrane potentials. Association of α subunits with both $\beta 1$ and $\beta 2$ subunits is sufficient to cause α subunits to gate nearly entirely in the fast mode. These common effects of the two subunits indicate that formation of the native heterotrimeric sodium channel complex promotes cell surface expression and fast gating as observed in mature neurons.

$\beta 2$ subunits have several properties that distinguish them from $\beta 1$ subunits. They are components of neuronal sodium channels, but not sodium channels from muscle tissues (Wollner et al., 1987). They are linked to α subunits by disulfide bonds (Messner and Catterall, 1985). A large intracellular pool of free α subunits is present in developing neurons, and disulfide linkage to $\beta 2$ subunits is correlated with appearance of sodium channels on the neuronal cell surface (Schmidt and Catterall, 1986, 1987). Evidently, the $\beta 1$ and $\beta 2$ subunits of sodium channels have separate functional roles in addition to their common effects on sodium channel gating mode.

A CAM Motif in $\beta 2$ Subunits

Our results show that $\beta 2$ subunits have two properties that are unique among ion channel subunits. First, they contain a CAM motif having an immunoglobulin domain with striking sequence similarity to contactin/F3. Contactin/F3 binds tenascin and related extracellular matrix proteins (Zinsch et al., 1992; Vaughan et al., 1994). Its extracellular domain contains six immunoglobulin-like repeats followed by two fibronectin repeats and a transmembrane segment or glycosylphosphatidylinositol membrane anchor (Ranscht, 1988; Gennarini et al., 1989). The first region of sequence similarity with $\beta 2$ subunits is located at the COOH-terminal end of the third immunoglobulin repeat of contactin/F3 (Gennarini et al., 1989), within a 45 kDa peptide fragment that has been shown to contain the tenascin-binding activity (Zinsch et al., 1992). The position of this sequence within the immunoglobulin fold is similar for contactin and $\beta 2$. Thus, this sequence in $\beta 2$ may be involved in interac-

tion with extracellular matrix proteins related to tenascin. In most cell types in intact tissues, ion channels are immobilized and concentrated in specific locations. For example, sodium channels are highly concentrated in nodes of Ranvier in myelinated axons and in axon hillocks. Interaction of the CAM motif on the $\beta 2$ subunit with extracellular matrix proteins may serve to immobilize sodium channels in nodes of Ranvier, axon hillocks, and other sites of high concentration in adult nervous tissue. The structure of $\beta 2$ may define a class of ion channel auxiliary subunits that have extracellular CAM motifs and are involved in immobilization of ion channels in muscle, endocrine, and epithelial tissues as well as in neurons.

Expansion of the Cell Surface Membrane by $\beta 2$ Subunits

The second unique property of $\beta 2$ is its ability to cause expansion of the cell surface membrane. Our capacitance measurements suggest that the surface area of the electrically contiguous cell surface membrane increases up to 4-fold in oocytes expressing $\beta 2$. Our electron microscopic results confirm that the surface area of the plasma membrane microvilli is greatly increased and suggest that the large increase in cell surface membrane results from fusion of intracellular membrane vesicles. After injection of high levels of $\beta 2$ RNA, the surface area of the microvilli is substantially expanded, while two major classes of intracellular vesicles, the cortical granules and the pigment granules, are greatly reduced in number. One intriguing hypothesis is that balanced expression of α and $\beta 2$ increases sodium channel expression by stimulating fusion of intracellular transport vesicles containing sodium channels with the plasma membrane. In contrast, excess concentrations of $\beta 2$ subunits may cause indiscriminant fusion of intracellular vesicles with the surface membrane of the oocyte, since both cortical granules and pigment granules are lost from the submembrane compartment.

Possible Role in Neuronal Development

Expression of $\beta 2$ subunit mRNA is detected in the earliest phase of neurogenesis in rat brain, and expression is greatly increased concomitant with axon extension and synaptogenesis. Migrating growth cones and axons, which contain sodium channels, are thought to undergo progressive interactions with surrounding cells and extracellular matrix (Goodman and Schatz, 1993). The striking similarity of the amino acid sequences of $\beta 2$ and the neuronal cell surface adhesion protein contactin/F3 suggests that the $\beta 2$ subunit may participate in cell–cell or cell–matrix interactions in development. Contactin/F3 is implicated in the regulation of neurite migration by interaction with tenascin (Pesheva et al., 1993). Contactin/F3 expression is developmentally regulated in a pattern similar to the $\beta 2$ mRNA with maximum expression in the mouse brain 1–2 weeks after birth during the period of rapid axon extension and synaptogenesis (Gennarini et al., 1989). These characteristics of contactin/F3 and the $\beta 2$ subunit suggest that they may both serve as points of contact between the axon membrane and the surrounding extra-

cellular matrix during axon extension and synapse formation.

Interaction of developing axons with oligodendrocytes during myelination has important effects on sodium channel regulation. Sodium channels are progressively localized to the nodes of Ranvier as myelination proceeds (Dugandzija-Novakovic et al., 1995). Disruption of myelination by deletion of the myelin basic protein gene in the shiverer mutant mouse causes a dramatic up-regulation of type II sodium channel expression in the hypomyelinated fibers in the central nervous system (Westenbroek et al., 1992). Oligodendrocytes express the tenascin homolog janusin, and the level of its expression is regulated by interactions with neurons (Jung et al., 1993). Therefore, interactions between the contactin homology domain of the β 2 subunit and tenascin in the extracellular matrix or tenascin-like proteins in the myelin sheath may play a role in these aspects of regulation of sodium channel localization and expression in myelinated axons.

Experimental Procedures

Purification and Amino Acid Sequence Analysis of the β 2 Subunit

Sodium channels were purified from rat brain (Hartshorne and Catterall, 1984), separated from α and β 1 subunits (Reber and Catterall, 1987; Messner and Catterall, 1986), further purified by SDS-PAGE, electroblotted to Immobilon PVDF membranes (Isom et al., 1992), and sequenced with an Applied Biosystems model 477A protein microsequencer. To generate peptide fragments, β 2 subunits were electroblotted to nitrocellulose, detected using Ponceau S, and digested in situ with trypsin or V8 protease (Aebersold et al., 1987; Isom et al., 1992). The cleavage fragments were separated by HPLC and subjected to amino acid sequencing.

Cloning of the β 2 Subunit cDNA

The initial β 2 cDNA was isolated by PCR from an oligo(dT)-primed rat brain library in λ ZAP II using degenerate oligonucleotides encoding residues 3–8 and 27–32 of peptide 5 as determined by amino acid sequencing (Isom et al., 1992). The predicted 90 bp cDNA was gel purified, isolated, and sequenced, and the sequence was extended by one PCR reaction primed with a degenerate oligonucleotide encoding residues 2–7 of peptide 1 and an exact oligonucleotide corresponding to the last 17 nucleotides of the 90 bp cDNA and a second PCR reaction primed with an exact oligonucleotide and the pBluescript primer KS. The two extended PCR products were subcloned into pBluescript SK(+), random prime labeled with 11-digoxigenin-dUTP, and used to screen duplicate lifts of the λ ZAP II rat brain cDNA library. A single clone (p β 2.8a-1) was positive with both probes. It was subcloned and sequenced in both directions on an Applied Biosystems 373A DNA Sequencer.

Cloning of Genomic DNA Encoding the β 2 Subunit

A fragment of the β 2 gene was isolated by PCR using DNA isolated from rat blood as template and oligonucleotides corresponding to the 5' and 3' ends of the β 2 coding sequence as primers. The resulting 1400 nt PCR product was gel purified, subcloned, and sequenced in both directions.

Expression in *Xenopus* Oocytes

The putative precursor form and the mature forms of β 2 were subcloned into the *Xenopus* expression vector pSP64T, linearized with EcoRI, and transcribed using the Ambion SP6 mMessage mMachine kit. Oocytes were isolated from pieces of ovary obtained from anesthetized female *Xenopus* frogs (*Xenopus* I, Ann Arbor, MI) by treatment for 3 hr in 1.5 mg/ml collagenase (Sigma, type I) dissolved in OR2 (82.5 mM NaCl, 2 mM KCl, 1 mM MgCl₂, 5 mM HEPES [pH 7.5]). Healthy stage 5–6 oocytes were transferred to Barth's medium (88 mM

NaCl, 1 mM KCl, 0.82 mM MgSO₄, 0.33 mM Ca(NO₃)₂, 0.41 mM CaCl₂, 2.4 mM NaHCO₃, 10 mM HEPES [pH 7.4]) supplemented with 50 μ g/ml gentamicin and 5% fetal bovine serum and injected on the day after isolation with 50 nl of RNA solution. Electrophysiological recording was performed 2–4 days after injection using two-microelectrode and cell-attached macropatch voltage-clamp methods (McPhee et al., 1995) at room temperature.

Electron Microscopy

Oocytes were processed for electron microscopy using a protocol similar to that described by Kelly et al. (1991). Thin sections were cut with a Reichart Om U2 ultramicrotome, collected on 200 parallel copper grids, stained with lead citrate, and examined with a Phillips 300 electron microscope at 80 kV.

Northern Blots

Total cellular RNA was purified using TRIzol reagent (GIBCO BRL, Gaithersburg, MD). Northern blot analysis of 10 μ g of each sample of total RNA was performed as described previously (Isom et al., 1995). A segment of the β 1 coding sequence (Isom et al., 1995) and a segment of the β 2 coding sequence corresponding to nucleotides 90–400 were used as a digoxigenin-labeled antisense cRNA probes (Isom et al., 1995). Equal loading of RNA on each gel lane was confirmed by analysis of ethidium bromide staining of the ribosomal RNA bands.

Acknowledgments

We thank Alice B. Brownstein, Carl Baker, and Hanna Ionis for expert technical assistance and Drs. Harry Charbonneau and Kenneth Walsh for assistance with amino acid sequence determination. This research was supported by National Institutes of Health Research Grant NS25704 to W. A. C., the W. M. Keck Foundation, and National Institutes of Health General Clinical Research Center Grant M01 RR00042 to the University of Michigan. Peptide synthesis and sequencing, oligonucleotide synthesis, and automated DNA sequencing were carried out in the Molecular Pharmacology Facility, Department of Pharmacology, University of Washington.

Received June 22, 1995; revised September 11, 1995.

References

- Aebersold, R.H., Leavitt, J., Saavedra, R.A., Hood, L.E., and Kent, S.B. (1987). Internal amino acid sequence analysis of proteins separated by one- or two-dimensional gel electrophoresis after *in situ* protease digestion on nitrocellulose. *Proc. Natl. Acad. Sci. USA* **84**, 6970–6974.
- Beckh, S., Noda, M., Lubbert, H., and Numa, S. (1989). Differential regulation of three sodium channel messenger RNAs in the rat central nervous system during development. *EMBO J.* **8**, 3611–3616.
- Bennett, P.B., Makita, N., and George, A.L., Jr. (1993). A molecular basis for gating mode transitions in human skeletal muscle sodium channels. *FEBS Lett.* **326**, 21–24.
- Cannon, S.C., McClatchey, A.I., and Gusella, J.F. (1993). Modification of the Na⁺ current conducted by the rat skeletal muscle α subunit by coexpression with a human brain β subunit. *Pflügers Arch.* **423**, 155–157.
- Catterall, W.A. (1992). Cellular and molecular biology of voltage-gated sodium channels. *Physiol. Rev.* **72**, S15–S48.
- Dayhoff, M.O., Barker, W.C., and Hunt, L.T. (1983). Establishing homologies in protein sequences. *Meth. Enzymol.* **91**, 524–545.
- De Jongh, K.S., Merrick, D.K., and Catterall, W.A. (1989). Subunits of purified calcium channels: a 212-kDa form of α -1 and partial amino acid sequence of an independent β subunit. *Proc. Natl. Acad. Sci. USA* **86**, 8585–8589.
- Dugandzija-Novakovic, S., Koszowski, A.G., Levinson, S.R., and Shrager, P. (1995). Clustering of Na⁺ channels and node of Ranvier formation in remyelinating axons. *J. Neurosci.* **15**, 492–503.
- Gennarini, G., Cibelli, G., Rougon, G., Mattei, M.G., and Goridis, C. (1989). The mouse neuronal cell surface protein F3: a phosphatidylyl-

sitol-anchored member of the immunoglobulin superfamily related to chicken contactin. *J. Cell Biol.* 109, 775–788.

Goodman, C.S., and Schatz, C.J. (1993). Developmental mechanisms that generate precise patterns of neuronal connectivity. *Neuron* 10, 77–98.

Gordon, D., Merrick, D., Wollner, D.A., and Catterall, W.A. (1988). Biochemical properties of sodium channels in a wide range of excitable tissues studied with site-directed antibodies. *Biochemistry* 27, 7032–7038.

Hartshorne, R.P., and Catterall, W.A. (1984). The sodium channel from rat brain: purification and subunit composition. *J. Biol. Chem.* 259, 1667–1675.

Hille, B. (1992). *Ionic Channels of Excitable Membranes* (Sunderland, Massachusetts: Sinauer).

Isom, L.L., De Jongh, K.S., Patton, D.E., Reber, B.F.X., Offord, J., Charbonneau, H., Walsh, K., Goldin, A.L., and Catterall, W.A. (1992). Primary structure and functional expression of the $\beta 1$ subunit of the rat brain sodium channel. *Science* 256, 839–842.

Isom, L.L., De Jongh, K.S., and Catterall, W.A. (1994). Auxiliary subunits of voltage-gated ion channels. *Neuron* 12, 1183–1194.

Isom, L.L., Scheuer, T., Brownstein, A.B., Ragsdale, D.S., Murphy, B.J., and Catterall, W.A. (1995). Functional co-expression of the $\beta 1$ and type IIA α subunits of sodium channels in a mammalian cell line. *J. Biol. Chem.* 270, 3306–3312.

Jung, M., Pesheva, P., Schachner, M., and Trotter, J. (1993). Astrocytes and neurons regulate the expression of the neural recognition molecule janusin by cultured oligodendrocytes. *Glia* 9, 163–175.

Kelly, G., Eib, D.W., and Moon, R.T. (1991). Histological preparation of *Xenopus laevis* oocytes and embryos. *Meth. Cell Biol.* 36, 389–417.

Kozak, M. (1986). Point mutations define a sequence flanking the AUG initiator codon that modulates translation by eukaryotic ribosomes. *Cell* 44, 283–292.

Krafte, D.S., Goldin, A.L., Auld, V.S., Dunn, R.J., Davidson, N., and Lester, H.A. (1990). Inactivation of cloned sodium channels expressed in *Xenopus* oocytes. *J. Gen. Physiol.* 96, 689–706.

Kyte, J., and Doolittle, R.F. (1982). A simple method for displaying the hydropathic character of the protein. *J. Mol. Biol.* 157, 105–132.

Levinson, S.R., Duch, D.S., Urban, B.W., and Recio-Pinto, E. (1986). The sodium channel from *Electrophorus electricus*. *Ann. NY Acad. Sci.* 479, 162–178.

Makita, N., Bennett, P.B., and George, A.L., Jr. (1994). Voltage-gated $\beta 1$ subunit mRNA expressed in adult human skeletal muscle, heart, and brain is encoded by a single gene. *J. Biol. Chem.* 269, 7571–7578.

McPhee, J.C., Ragsdale, D.S., Scheuer, T., and Catterall, W.A. (1995). A critical role for transmembrane segment IVS6 of the sodium channel α subunit in fast inactivation. *J. Biol. Chem.* 270, 12025–12034.

Messner, D.J., and Catterall, W.A. (1985). The sodium channel from rat brain: separation and characterization of subunits. *J. Biol. Chem.* 260, 10597–10604.

Messner, D.J., and Catterall, W.A. (1986). The sodium channel from rat brain: role of the $\beta 1$ and $\beta 2$ subunits in saxitoxin binding. *J. Biol. Chem.* 261, 211–215.

Moorman, J.R., Kirsch, G.E., Van Dongen, A.M.J., Joho, R.H., and Brown, A.M. (1990). Fast and slow gating of sodium channels encoded by a single mRNA. *Neuron* 4, 243–252.

Patton, D.E., Isom, L.L., Catterall, W.A., and Goldin, A.L. (1994). The adult rat brain $\beta 1$ subunit modifies activation and inactivation gating of multiple sodium channel α subunits. *J. Biol. Chem.* 269, 17649–17655.

Pesheva, P., Gennarini, G., Goridis, C., and Schachner, M. (1993). The F3/F11 cell adhesion molecule mediates the repulsion of neurons by the extracellular matrix glycoprotein J1-160/180. *Neuron* 10, 69–72.

Qu, Y., Isom, L.L., Westenbroek, R.E., Rogers, J.C., Tanada, T., McCormick, K.A., Scheuer, T., and Catterall, W.A. (1995). Modulation of cardiac Na^+ channel expression in *Xenopus* oocytes by $\beta 1$ subunits. *J. Biol. Chem.*, in press.

Ranscht, B. (1988). Sequence of contactin, a 130-kd glycoprotein concentrated in areas of interneuronal contact, defines a new member of the immunoglobulin supergene family in the nervous system. *J. Cell Biol.* 107, 1561–1573.

Reber, B.F.X., and Catterall, W.A. (1987). Hydrophobic properties of the $\beta 1$ and $\beta 2$ subunits of the rat brain sodium channel. *J. Biol. Chem.* 262, 11369–11374.

Scheinman, R.I., Auld, V.J., Goldin, A.L., Davidson, N., Dunn, R.J., and Catterall, W.A. (1989). Developmental regulation of sodium channel expression in the rat forebrain. *J. Biol. Chem.* 264, 10660–10666.

Schmidt, J.W., and Catterall, W.A. (1986). Biosynthesis and processing of the α subunit of the voltage-sensitive sodium channel in rat brain neurons. *Cell* 46, 437–445.

Schmidt, J.W., and Catterall, W.A. (1987). Palmitoylation, sulfation, and glycosylation of the α subunit of the sodium channel: role of post-translational modification in channel assembly. *J. Biol. Chem.* 262, 13713–13723.

Tong, J., Potts, J.F., Rochelle, J.M., Seldin, M.F., and Agnew, W.S. (1993). A single $\beta 1$ subunit mapped to mouse chromosome 7 may be a common component of Na^+ channel isoforms from brain, skeletal muscle and heart. *Biochem. Biophys. Res. Commun.* 195, 679–685.

Vaughan, L., Weber, P., D'Alessandri, L., Zisch, A.H., and Winterhalter, K.H. (1994). Tenascin-contactin/F11 interactions: a clue for a developmental role? *Perspect. Dev. Neurobiol.* 2, 43–52.

Westenbroek, R.E., Noebels, J.L., and Catterall, W.A. (1992). Elevated expression of type IIA sodium channels in hypomyelinated axons of shiverer mouse brain. *J. Neurosci.* 12, 2259–2267.

Wickner, W.T., and Lodish, H.F. (1985). Multiple mechanisms of protein insertion into and across membranes. *Science* 230, 400–407.

Williams, A.F., and Barclay, A.N. (1988). The immunoglobulin superfamily domains for cell surface recognition. *Annu. Rev. Immunol.* 6, 381–405.

Wollner, D.A., Messner, D.J., and Catterall, W.A. (1987). $\beta 2$ subunits of sodium channels from vertebrate brain: studies with subunit-specific antibodies. *J. Biol. Chem.* 262, 14709–14715.

Wollner, D.A., Scheinman, R., and Catterall, W.A. (1988). Sodium channel expression and assembly in the retinal ganglion cell. *Neuron* 1, 727–737.

Zhou, J., Potts, J.F., Trimmer, J.S., Agnew, W.S., and Sigworth, F.J. (1991). Multiple gating modes and the effect of modulating factors on the $\mu 1$ sodium channel. *Neuron* 7, 775–785.

Zisch, A.H., D'Alessandri, L., Ranscht, B., Falchetto, R., Winterhalter, K.H., and Vaughan, L. (1992). Neuronal cell adhesion molecule contactin/F1 binds to tenascin via its immunoglobulin-like domains. *J. Cell Biol.* 119, 203–213.

GenBank Accession Numbers

The accession numbers for the sequences reported in this paper are U37026 and U37147.